Capillarity

Vol. 14, No. 3, p. 82-99, 2025

Original article

Numerical and semi-analytical modelling of the capillary end effect for porous media of any wettability state

Saleh Goodarzian*, K. S. Sorbie

Institute of GeoEnergy, Heriot-Watt University, Edinburgh, EH14 4AS, Scotland, UK

Keywords:
Water outflow
capillary end effect
exit saturation
modified IMPES method

Cited as:
Goodarzian, S., Sorbie, K. S. Numerical and semi-analytical modelling of the capillary end effect for porous media of any wettability state. Capillarity, 2025, 14(3): 82-99.
https://doi.org/10.46690/capi.2025.03.03

Abstract:
The capillary end effect appears in a two-phase displacement process as a physical consequence of the capillary discontinuity at the system outlet and causes accumulation of the wetting phase at this location and back along the system. In the study of water injection into a one-dimensional system, to obtain accurate phase saturation profiles in the presence of the capillary end effect at any time during the transient state, conventional implicit pressure explicit saturation and one-dimensional convection-diffusion methods have been modified by applying a novel boundary condition. This modification is entirely physics-based, whereas in commercial simulators fix-up procedures are applied which do not conserve mass. A new term "exit saturation" is introduced which provides a useful way to study and analyse the capillary end effect. Transient-state flow development in the presence of the capillary end effect in different wetting systems is presented in detail in this work. Also, several methods are presented to obtain steady-state saturation profiles. At steady-state conditions, the capillary end effect vanishes in purely water-wet systems and all oil in principle can be displaced from the system in a finite, but very long time. However, in mixed- and oil-wet systems, some oil is permanently trapped in the system at any chosen flowrate, i.e., the capillary end effect cannot be entirely removed no matter how large the flowrate is. However, oil recovery is improved by increasing the flowrate.

1. Introduction

In the water injection displacement process into a one-dimensional (1D) porous medium, capillary pressure follows a function inside the system for any wettability state and suddenly becomes zero at the system outlet. This capillary pressure discontinuity can distort phase saturation profiles within the system and is called the *Capillary End Effect* (CEE). Depending upon the system wettability (represented by the sign of capillary pressure in this work), the following scenarios may be encountered. Note that only water is injected into the system and there is no counter-current flow anywhere in the system.

In water-wet systems, capillary pressure is positive inside the system (while being zero at the outlet), therefore a negative capillary pressure gradient develops which prevents water from flowing out. Negative capillary pressure gradient actually hinders water outflow. As a result, water accumulates at the end of the system. Leverett (1941) first presented a clear explanation of this physical phenomenon. How far this accumulation extends back into the system depends on the magnitude of the capillary pressure, petrophysical properties and flow conditions. In oil-wet systems, capillary pressure is negative inside the system, therefore a positive capillary pressure gradient develops at the end of the system. In this case both viscous pressure gradient and capillary pressure gradient contribute to water flow which results in depletion of water at

*Corresponding author.
E-mail address: saleh.goodarzian@hw.ac.uk (S. Goodarzian); ken.sorbie@hw.ac.uk (K. S. Sorbie).

Yandy Scientific Press

2709-2119
Received February 5, 2025; revised February 27, 2025; accepted March 15, 2025; available online March 19, 2025.

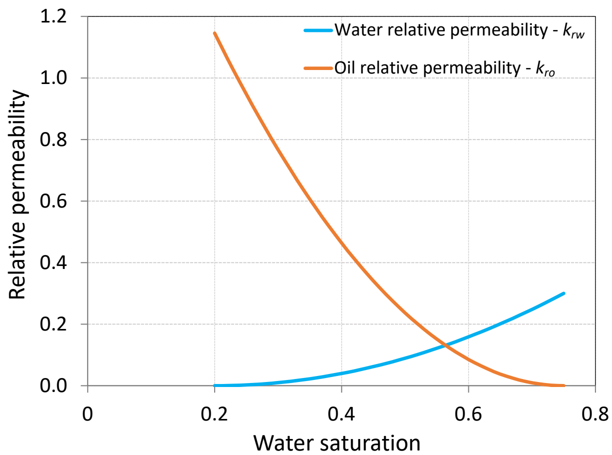

Fig. 1. Water and oil relative permeability functions used in this study (as in Eq. (1)).

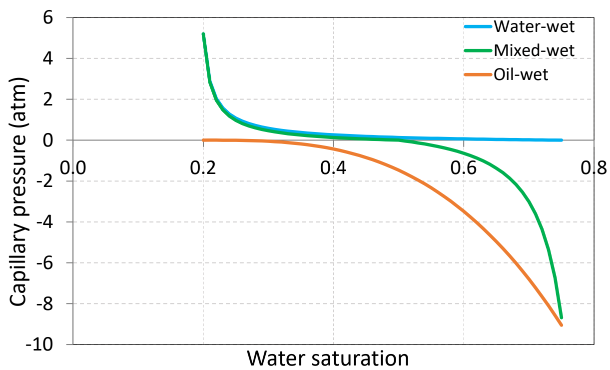

Fig. 2. Capillary pressure function used in this study (as in Eq. (1)).

the end of the system. In mixed-wet systems, both behaviors are observed which will be explained in detail below. The primary focus of this paper is to study the CEE and numerically show how flow develops in different wetting systems in the presence of the CEE.

Many researchers have theoretically obtained the water saturation profile along the system at steady-state conditions in different wetting systems. Richardson et al. (1952) presented a theoretical method to obtain oil saturation profile along the system during a drainage process (oil being displaced by gas) at steady-state conditions. Hadley and Handy (1956) also provided formulas for calculating steady-state saturation and pressure profiles during the displacement process in the presence of the CEE. Kyte and Rapoport (1958) explained that the CEE at the end of the system holds water from production and delays breakthrough time which results in more oil recovery prior to water breakthrough.

Not considering the CEE in the calculations (using the results of steady-state experiments) gives erroneous two-phase relative permeabilities, then it is important to find ways to alleviate or entirely remove this effect. Virnovsky et al. (1995, 1998) proposed a multi-rate steady-state relative permeability experiment and used simulations to correct relative permeability data for the CEE. Gupta and Maloney (2014) introduced the Intercept Method to entirely remove the CEE from steady-

Table 1. System properties and flow conditions for simulation runs for the base case data.

Reservoir properties and flow conditions	Value	Unit
Length in x-direction, L	10	cm
Length in y-direction, Δy	4	cm
Length in z-direction, Δz	4	cm
Porosity, ϕ	0.22	-
Oil viscosity, μ_o	20	cP
Water viscosity, μ_w	0.5	cP
Connate water saturation, S_{wc}	0.2	-
Residual oil saturation, S_{or}	0.25	-

state experimental results. Nazari and Jamiolahmadi (2019) pointed out the wrong assumptions in Gupta and Maloney's work and presented a different method to remove the CEE from the experimental data. The authors recently presented a rigorous analysis of "the CEE removal" methods to obtain correct relative permeabilities (Goodarzian and Sorbie, 2020, 2023; Goodarzian, 2021).

The experimental findings of Masalmeh (2012) give good confirmation of the theoretical understanding of the CEE problem proposed here (which will be discussed in this paper). However, literature lacks a robust method to handle the point of capillary pressure discontinuity at the end of the core to enable us to quantify the amount of water accumulation and depletion at the end of different wetting systems at any chosen time during the transient state. In this paper, the following questions are addressed, and explanations are substantiated by detailed mathematical analysis and numerical simulations.

1) How should the conventional Implicit Pressure Explicit Saturation (IMPES) and 1D convection-diffusion formulations be modified to capture the point of capillary pressure discontinuity at the end of the system, and hence obtain the water saturation profile at any time during the transient state and at steady-state conditions?
2) Is the practice of taking dummy grid-blocks with zero capillary pressure at the end of the system to represent the outlet accurate or even necessary? If so, how many dummy grid-blocks are necessary?
3) Can the use of Local Grid Refinement (LGR) in a numerical simulation help (or work) to more accurately represent the transient saturation profiles in the presence of the CEE?
4) Does the new formulation introduced in this work guarantee mass balance, and can it be applied to give accurate results in mixed- and oil-wet systems?
5) Can the proposed modification give the final water saturation profile (with trapped oil in mixed- and oil-wet systems) at steady-state conditions as it can directly be obtained by semi-analytical methods?

In this work, the following relative permeability and capillary pressure functions (Eq. (1) or Figs. 1 and 2), system

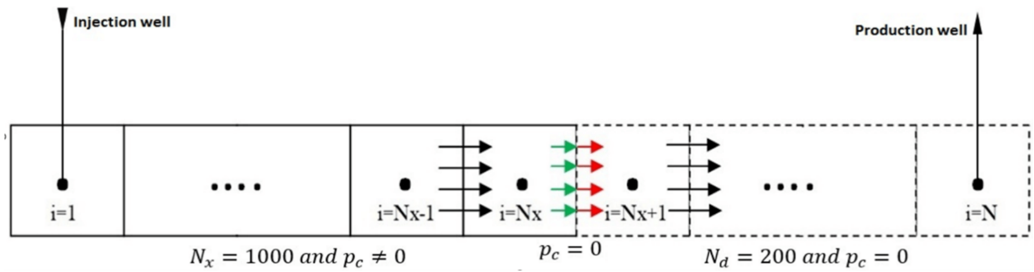

Fig. 3. A schematic view of real and dummy grid-blocks and the point of capillary discontinuity in the water injection (incompressible) displacement process.

properties and flow conditions (Table 1) are used. Note that the three wetting systems in this study share the same input data, and they only differ in capillary pressure as shown in Eq. (1) and Fig. 2. All the data here is entirely arbitrary and for illustration purposes only and they are not from a specific core. Capillary pressure for water-wet systems is always positive to indicate rock's tendency to pull water in. Oil-wet capillary pressure is always negative to indicate rock's tendency to expel water and there must be a pressure to push water in the oil-wet core. Mixed-wet system capillary pressure shows both properties. This arbitrary dataset is primarily chosen just to show the behaviour of the phase saturation and pressure regime along different wetting systems in the presence of the CEE. Also, it was meant to make it less complicated and easy to follow:

$$\begin{aligned} k_{rw} &= 0.9917(S_w - S_{wc})^2 \\ k_{ro} &= 3.7867(1 - S_w - S_{or})^2 \\ p_{c,waterwet} &= \frac{0.136054}{(S_w - S_{wc} + 0.01)^{0.8}} - 0.216353 \\ p_{c,mixedwet-positive\ \ part} &= \frac{0.139567}{(S_w - S_{wc} + 0.01)^{0.8}} - 0.356204 \\ p_{c,mixedwet-negative\ \ part} &= \frac{-0.139567}{(2S_{wa} - S_w - S_{wc} + 0.01)^{1.5}} + 0.808639 \\ p_{c,oilwet} &= -54.42177(S_w - S_{wc})^3 \end{aligned} \tag{1}$$

For the standard model of two-phase (oil/water) flow, governing flow equations are well-known and may be expressed in different well-known formulations, such as the coupled saturation/pressure equation or the two-phase convection/capillary dispersion formulation (Peaceman, 1977; Aziz and Settari, 1979; Stephen et al., 2001; Pinder and Gray, 2008). In this work, the two-phase flow equations in already discretized form within the IMPES formulation are used. The CEE problem is essentially a boundary condition problem, and it turns out that this problem can be analyzed most straightforwardly from the discretized form. In addition, this leads us to some semi-analytic expressions for calculating the exit saturation (explained below) at the grid scale and for calculating the steady-state saturation profiles showing oil trapping for the oil- and mixed-wet cases. Thus, starting from the discretized equations is a very fruitful approach for analysing the CEE problem.

2. Solution scheme for the CEE problem

In this water injection process, an incompressible displacement is assumed which means the total flowrate at each cross section is fixed and equal to the water injection rate in the first grid-block. To solve the CEE problem, the concept of flux continuity (van Duijn and de Neef, 1998) at the point of capillary pressure discontinuity at the system outlet is employed. Before water reaches the last real grid-block, only oil flows out of the system. When water reaches the outlet then, for some time, the negative capillary pressure gradient is too large to allow water outflow, hence only oil flows out of the system. When only oil flows out of the system, the oil flux continuity formulation must be used. As water saturation increases with time, capillary pressure at the end of the core reduces. Hence, rock loses its ability to hold water back in the system, then at some point two-phase flow is established, for which the total flux continuity formulation must be used. In the IMPES formulation, water outflow at any time is given by Eq. (2). When it is negative or zero, oil flux continuity formulation, and when positive, total flux continuity formulation must be used. Refer to the Appendix for more details of the modification introduced here:

$$\begin{aligned} q_{w,out} &= \frac{\Delta y \Delta z}{0.5\Delta x}(k\lambda_w)_{N_x,1}\left[p^{n+1}_{w,N_x,1} - p^{n+1}_{wb}\right] \\ &= \frac{\Delta y \Delta z}{0.5\Delta x}(k\lambda w)_{N_x,1}\left[(p^{n+1}_{o,N_x,1} - p^{n}_{c,N_x,1}) - (p^{n+1}_{ob} - p_{cb})\right] \\ &= \frac{\Delta y \Delta z}{0.5\Delta x}(k\lambda w)_{N_x,1}\left[(p^{n+1}_{o,Nx,1} - p^{n+1}_{ob}) + (p_{cb} - p^{n}_{c,Nx,1})\right] \end{aligned} \tag{2}$$

where k is the absolute permeability, λ_w is the water mobility (i.e., k_{rw}/μ_w), p_{cb} is the capillary pressure at the outlet which is zero (or any value), p_{ob} is the oil-phase pressure at the boundary between the last real grid-block and the first dummy grid-block, n denotes the current timestep and $n+1$ denotes the next time step. In Fig. 3, a schematic view of the system is presented. There are N_x real grid-blocks and $N_d = N - N_x$ dummy grid-blocks, shown by solid and dashed lines, respectively.

To solve the problem of the CEE, the physics of flow at the point of capillary discontinuity is introduced into the numerical simulation. The point of capillary discontinuity is not simply replaced by a dummy grid-block with zero capillary pressure. Proper equations must be developed to capture the very outlet point. This outlet point with zero capillary pressure must be

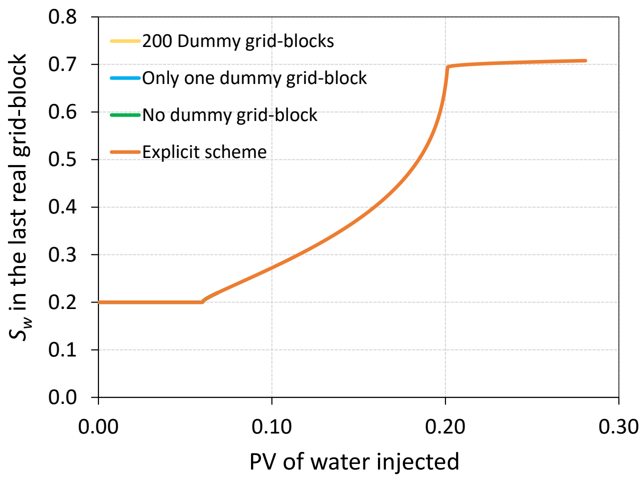

Fig. 4. Water saturation in the last real grid-block of the system (PV$=0.28075$ and $V_r=\mu_o/\mu_w=40$).

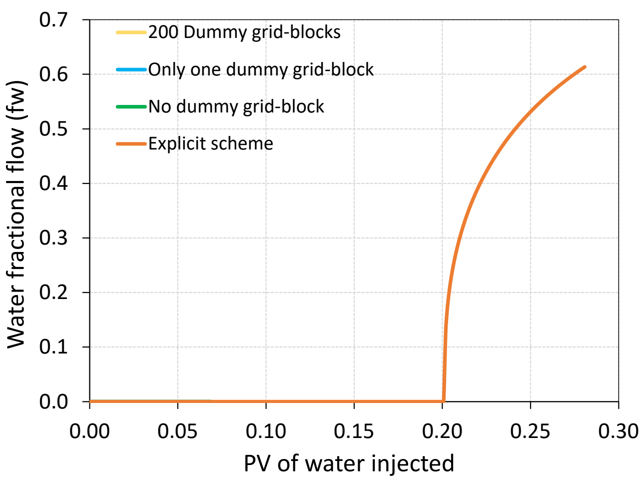

Fig. 5. Water fractional flow from the system (PV$=0.28075$ and $V_r=40$).

an active player in the equations. LGR does not solve the problem either because merely taking smaller grid-blocks near the outlet does not add physics to the solution of the problem. LGR only better represents the saturation profile but does not ensure mass conservation because mass conservation is guaranteed only when correct equations are used in the solution. The proposed modification guarantees mass conservation to machine accuracy. It must be stated that this formulation is only suitable when there is a capillary discontinuity at the system outlet or inside heterogeneous systems.

3. Comparison of results obtained from various modelling methods

Four schemes for the numerical solution of the CEE problem are presented here (with technical details in the Appendix, containing demonstrative Figs. A1, A2, and A3):

1) With 200 dummy grid-blocks (using the modified IMPES method),
2) With only one dummy grid-block (using the modified IMPES method),

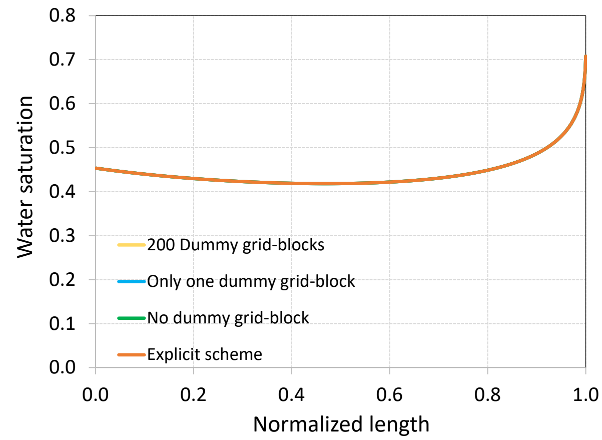

Fig. 6. Water saturation along the system (at PV$=0.28075$ and $V_r=40$).

3) With no dummy grid-blocks (using the modified IMPES method),
4) With no dummy grid-blocks (using the modified 1D convection-diffusion equation).

Note that dummy and real grid-blocks are initialized the same way, with the same permeability, porosity and relative permeability. The only difference is that capillary pressure is zero in dummy grid-blocks. Also note that capillary pressure at the boundary between real and dummy grid-blocks is always zero (Fig. 3).

The first simulation example using the data in Eq. (1) and Table 1 for the water-wet case (with $k=518$ mD and $q=0.02$ cc/s) shows the build-up of water saturation in the last real grid-block, $S_{w,N_x,1}$, vs. PV of water injected in Fig. 4. Water-cut vs. PV of water injected is shown in Fig. 5 and the water saturation profile at a given time (PV$=0.28075$) is shown in Fig. 6. The results obtained from all 4 schemes are identical and mass is perfectly conserved during the displacement process. This demonstrates that to capture the CEE, no dummy grid-block is needed at all. Only the correct flux continuity condition must be applied, as explained above. Even if dummy grid-blocks are used, then the correct equations for flow of each phase to/from the boundary point are still required, and this is clearly sufficient. The practice of using dummy grid blocks within the conventional IMPES formulation to "resolve" the CEE is both **unnecessary and incorrect** since it gives erroneous results and does not conserve mass.

4. Verification of the new boundary flux conditions

Water outflow within the conventional IMPES formulation is the following:

$$q_{w,out}=\frac{\Delta y\Delta z}{\Delta x}\left(k\lambda_w\right)_{N_x,1}\left[\left(p^{n+1}_{o,N_x,1}-p^{n+1}_{o,N_x+1,1}\right)+\left(p^{n}_{c,N_x+1,1}-p^{n}_{c,N_x,1}\right)\right] \tag{3}$$

Before water reaches grid-block $i=N_x$, saturation is at connate water saturation at which water mobility is zero (since water relative permeability is zero), hence there is zero outflow of water. After water enters this grid-block, the capillary pre-

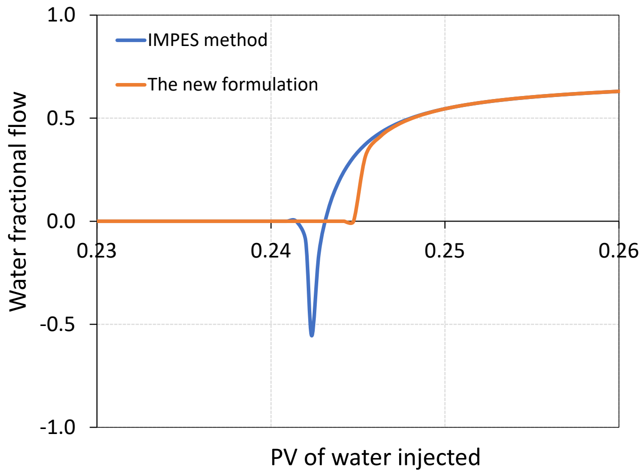

Fig. 7. Water fractional flow form the last real grid-block.

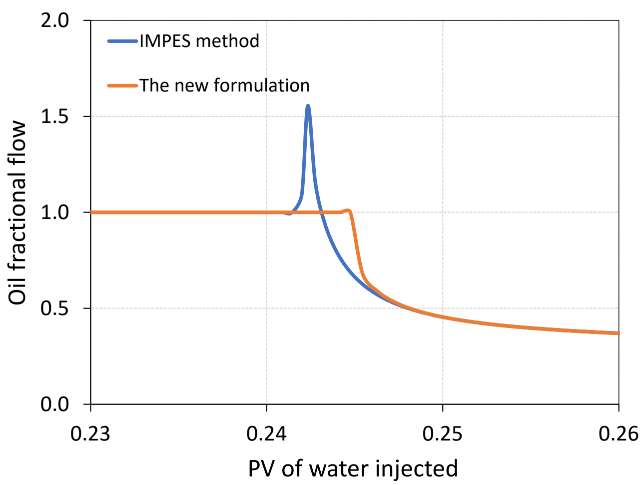

Fig. 8. Oil fractional flow from the last real grid-block.

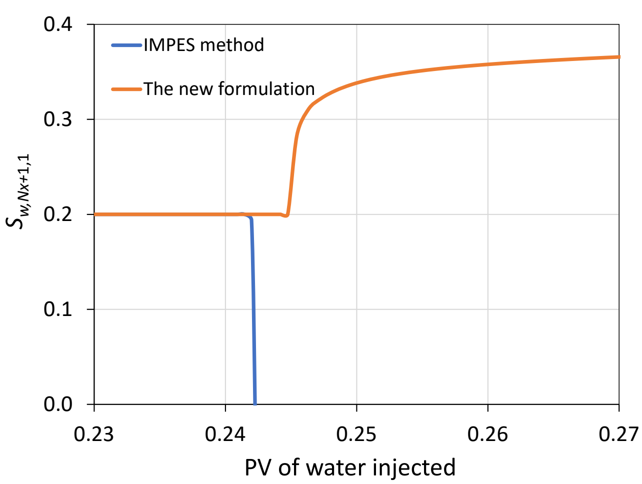

Fig. 9. Water saturation in the first dummy grid-block.

ssure difference is high and viscous pressure difference between two grid-blocks ($i = N_x$ and $i = N_x + 1$) is relatively low, therefore water outflow becomes negative. This means that a negative amount of water leaves grid-block $i = N_x$ and enters grid-block $i = N_x + 1$.

To maintain a fixed total flowrate (equal to the injection rate), oil has to flow out at a rate larger than the injection rate, which violates the physics of the incompressible displacement process. Negative water outflow leads to the following, which are all against the physics of flow and causes mass balance errors.

- Water saturation in grid-block $i = N_x + 1$ goes below connate water saturation,
- Water saturation in grid-block $i = N_x$ goes higher than it should due to negative water outflow which acts like inflow of water into this grid-block in reverse direction.

A simulation example with the data in Eq. (1) and Table 1 for the water-wet case (with $k = 290$ mD to emphasize the CEE and $q = 2.8$ cc/s) is considered in the conventional IMPES calculation, when water reaches the last real grid-block.

- Water outflow becomes negative (the blue curve in Fig. 7). However, in this new methodology, water outflow will never be negative (the orange curve in Fig. 7), as required physically.
- Oil outflow from grid-block $i = N_x$ goes above the injection rate, which is not physically correct (the blue curve in Fig. 8) since it must be equal to the injection rate up until a two-phase flow is established, as found using the new formulation and shown in Fig. 8 (by the orange curve).
- Water saturation in grid-block $i = N_x + 1$ (the blue curve in Fig. 9) goes below connate water saturation and becomes even negative due to the negative amount of water transported into this grid-block. This faulty result is not seen in the orange curve obtained from the new formulation.

4.1 Comparison of the new formulation with commercial numerical simulators

CMG and ECLIPSE use Adaptive-Implicit methods, in which grid-blocks that experience rapid changes in primary variables (e.g. pressure or saturation) are treated fully implicitly, but grid-blocks with small changes are handled in an IMPES fashion. In the case above (before water breakthrough), CMG uses fully implicit scheme, which is a numerical technique that calculates relative permeability and capillary pressure at the current timestep. This merely numerical technique does not incorporate the physics of the problem at the outlet with zero capillary pressure. Therefore, there will be a negative water outflow as soon as water reaches the last real grid-block which means water saturation in the first dummy grid-block will go below connate water saturation or even becomes negative, exactly as in the conventional IMPES method. On finding that CMG and ECLIPSE gave a discrepancy from the exact results obtained from the proposed formulation, it is speculated that they had applied a fix-up procedure to address this error. It appeared that, when the water saturation in the first dummy grid-block (and others) went below connate water saturation, then it was automatically reset to the connate water saturation. To confirm this conjecture, a command is used in the conventional IMPES code to do exactly this.

The water saturation profile obtained in this way (using

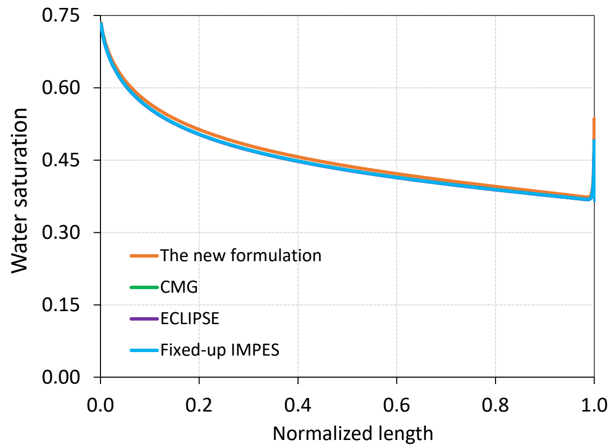

Fig. 10. Water saturation profiles obtained from four methods.

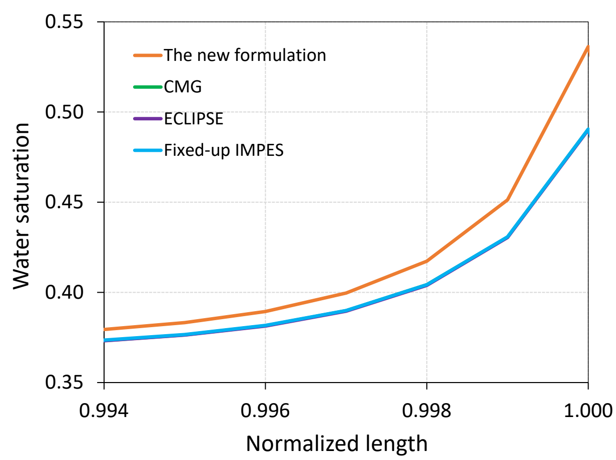

Fig. 11. A close-up view of water saturation profile at the system outlet in Fig. 10.

this fix-up procedure) is identical to the profiles given by CMG and ECLIPSE (Figs. 10 and 11), which are slightly different from the water saturation profile obtained from the proposed method, which is proven to be exact. Note that $x = 1$ denotes end of the real system, after which dummy grid-blocks are used.

At any point during the displacement process, the amount of injected water must be equal to the total amount of water produced from the production well and water remaining inside the system. Mass balance check is an important way to assess the accuracy of the numerical simulation scheme. For the case above, the error in the results given by CMG is 0.05% and by ECLIPSE is 0.12%, while it is $1.6 \times 10^{-13}\%$ (machine accuracy) in the proposed method. CMG and ECLIPSE give accurate results for "practical" purposes, but their solution schemes are not based on the correct physics of the problem. Applying the proposed modifications, the results obtained are accurate to machine accuracy.

5. The exit saturation, $S_{w,exit}$

The implementation of the correct CEE flux condition leads to a definition of and a semi analytical method for the accurate (i.e., exact) calculation of a quantity called exit saturation, denoted as $S_{w,exit}$. Exit saturation is the maximum water saturation in the last real grid-block (of size Δx) at which still only oil flows through the outlet. Note that this value is the volume average water saturation in the last real grid-block. As soon as water saturation goes beyond $S_{w,exit}$, water just starts flowing out and two-phase flow is established at the outlet. When $q_{w,out} = 0$, the following equation holds:

$$q_{w,out} = \frac{\Delta y \Delta z}{0.5\Delta x}(k\lambda_w)_{N_x,1}\left(p^{n+1}_{o,N_x,1} - p^{n+1}_{ob} + p_{cb} - p^{n}_{c,N_x,1}\right) = 0 \tag{4}$$

$p^{n+1}_{o,N_x,1} - p^{n+1}_{ob} + p_{cb} - p^{n}_{c,N_x,1}$ must be zero for this equation to hold, for other terms being non-zero. Applying the Darcy's law and knowing only oil flows at a rate equal to the injection rate, then:

$$p^{n+1}_{o,N_x,1} - p^{n+1}_{ob} = \frac{q_t\mu_o\dfrac{\Delta x}{2}}{kAk_{ro}(S_w)} = p^{n}_{c,N_x,1}(S_w) - p_{cb} \tag{5}$$

where $p_{cb} = 0$ (or any specified value). q_t is used here because water outflow is the same as total injection rate (no oil outflow yet). Then, Eq. (5) leads to the following equation:

$$F(S_w) = \frac{q_t\mu_o\dfrac{\Delta x}{2}}{kAk_{ro}(S_w)} - p_{c,N_x,1}(S_w) = 0 \tag{6}$$

Solving this **implicit** equation for S_w by the Newton-Raphson method gives the exit saturation. Inspection of Eq. (6) shows that as water saturation rises in this grid-block, viscous pressure difference term increases because oil relative permeability decreases while still oil flows out of this grid-block at a rate equal to the injection rate. At the same time, capillary pressure, i.e., $p^{n}_{c,N_x,1}(S_w)$ decreases when water saturation increases. Exit saturation is the point at which these two curves cross. Exit saturation can also be found using direct numerical simulation (i.e., the modified IMPES method).

Considering the water-wet system above (with $k = 220$ mD and $q = 8.50$ cc/s), Fig. 12 shows the red curve plotting the viscous pressure difference across the second half of the last real grid-block ($= p^{n+1}_{o,N_x,1} - p^{n+1}_{ob}$) and the blue curve plotting the capillary pressure in the last real grid-block, both vs. water saturation. The modified IMPES method gives $S_{w,exit} = 0.3499$ whereas implicit solution of Eq. (6) using the Newton-Raphson method gives $S_{w,exit} = 0.3449$. This slight difference is because Eq. (6) updates capillary pressure and oil relative permeability values with respect to water saturation at the current timestep (as this equation has no time term, hence previous time-step has no meaning for this equation and such information is not available), but in the IMPES method, pressure is solved with these values calculated in the previous timestep. This agreement can be made more accurate simply by taking smaller timesteps in the IMPES formulation so that capillary pressure and water/oil relative permeability values are calculated successively closer to the current timestep.

5.1 Effect of various parameters on the value of $S_{w,exit}$

It is straightforward to predict the effect of various parameters (q_t, μ_o, Δx and k) on $S_{w,exit}$ from Eq. (6) by comparing the terms in the related equality, $(qt\mu_o\Delta x/2)/kAk_{ro}(S_{w,exit}) =$

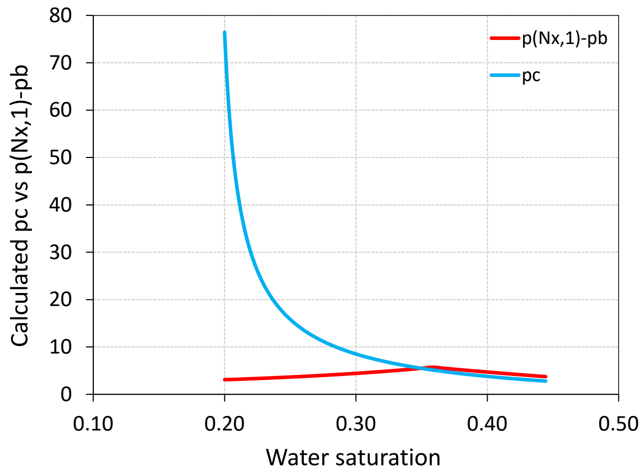

Fig. 12. Viscous pressure difference and capillary pressure vs. water saturation in the last real grid-block (base case).

$p_{c,N_x,1}(S_{w,exit})$. At higher q_t or μ_o, oil viscous pressure gradient is higher which overcomes the negative capillary pressure gradient before water is highly accumulated, hence lower $S_{w,exit}$. Also, by looking the equality, k_{ro} must be higher to maintain the equality, which means lower $S_{w,exit}$, which means less significant extent of the CEE into the system.

At a higher permeability, the opposite takes place. Oil viscous pressure gradient will be lower; therefore, water must reach higher saturations so that oil viscous pressure gradient is strong enough to overcome the negative capillary pressure gradient, hence more water accumulation in the last real grid-block and higher $S_{w,exit}$. Also, by looking the equality, k_{ro} must be lower to maintain the equality, which again means higher $S_{w,exit}$. It is less intuitive that a higher permeability leads to a more significant CEE that extends farther back into the system. This has been confirmed by the experimental results reported by Masalmeh (2012).

It is worthwhile noting that the exit saturation has no dependence on water viscosity, although water viscosity does affect the height of the saturation flood front. When a stronger water- or mixed-wet capillary pressure function (with all other parameters kept fixed) is used, the CEE will obviously be more significant.

It is important to note that exit saturation is the volume average water saturation in the last real grid-block when water just starts flowing out, but it does not mean that water saturation is the same all over the last real grid-block. To better see the water saturation profile in the near vicinity of the outlet, the LGR can be used. According to Eq. (6), exit saturation is higher in finer grids (i.e., lower Δx). As the grid size tends to zero ($\Delta x \to 0$), then exit saturation tends to $1-S_{or}$. Therefore, water saturation rises in the vicinity of the outlet. But no matter how small the grid is, exit saturation can never be exactly $1-S_{or}$ because in that case the Right Hand Side (RHS) of the equality above will be zero (since $p_c(1-S_{or})=0$), while the left hand side (LHS) is always a positive value, which cannot be correct. Therefore, there will be no volume inside the system with this saturation. This explains the apparent paradox of how oil can flow out of a water-wet system when the water saturation at the outlet is $1-S_{or}$ for which oil relative permeability is zero.

To summarize, when two-phase flow initiates and for the rest of the displacement process, water saturation rises in the vicinity of the outlet and is only asymptotically $1-S_{or}$ right at the outlet, where the capillary pressure is zero. Saturation is defined for a volume, not a point and there is no volume with this saturation in the system, hence two-phase flow can exist all over inside the system and from the system.

5.2 Exit saturation in mixed- or oil-wet systems

In a **mixed-wet core**, exit saturation is always lower than the value at which capillary pressure becomes zero ($p_c=0$ at $S_w=0.5$ in this study; see Fig. 2). At $S_w=0.5$, the RHS of the equality $(qt\mu_o\Delta x/2)/kAk_{ro}(S_{w,exit}) = p^n_{c,N_x,1}(S_{w,exit})$ is zero, while the LHS of the equation is always positive. Therefore, $S_w=0.5$ as the value of exit saturation is impossible. Assuming exit saturation being a value greater than 0.5, then the RHS of the equality will be negative while the LHS can never be negative. Therefore, in this work, exit saturation is always lower than 0.5 and for the calculation of the exit saturation in mixed-wet systems, only the positive leg of the capillary pressure function is required. Using the same argument above as for the water-wet case, when water just starts flowing out, water saturation in the vicinity of the outlet gradually increases to 0.5 (or any value at which $p_c=0$). As the displacement continues, water saturation in the whole system goes above 0.5. From this point onwards, water saturation in the vicinity of the outlet gradually drops to 0.5. When two-phase flow is established and for the rest of the displacement process, water saturation in the vicinity of the outlet approaches 0.5, either by gradual increase or gradual decrease (see plots "f, g and h" in Fig. 14) and is asymptotically 0.5 right at the outlet.

In an oil-wet core, when water reaches the last real grid-block, capillary pressure takes a negative value which creates a positive capillary pressure gradient at the end of the system that favours water flow. This tendency creates a region with depleted water as water outflow is favoured. Water saturation in the vicinity of the outlet gradually drops to S_{wc} (at which $p_c=0$) as soon as two-phase flow is established and for the rest of the displacement process and is asymptotically S_{wc} right at the outlet.

All the sensitivities to the parameters (q_t, μ_o, Δx and k) and the behaviour as $\Delta x \to 0$ have been verified by direct numerical simulation but these are not presented here; they are given in Goodarzian (2021).

6. Flow development in different wetting systems in the presence of the CEE

Water-, mixed- and oil-wet systems, in this work, differ only in the form of their capillary pressure functions (see Fig. 2 given by Eq. (1). To better understand the transient flow development, four distinct stages are considered; a) before breakthrough, b) peak generation (if it occurs), c) when exit saturation is reached and d) peak evolution after water breakthrough and late-time behavior. In Figs. 13, 14 and 15, it is shown how the saturation profile develops in water-, mixed- and oil wet systems, respectively. The core data is given in

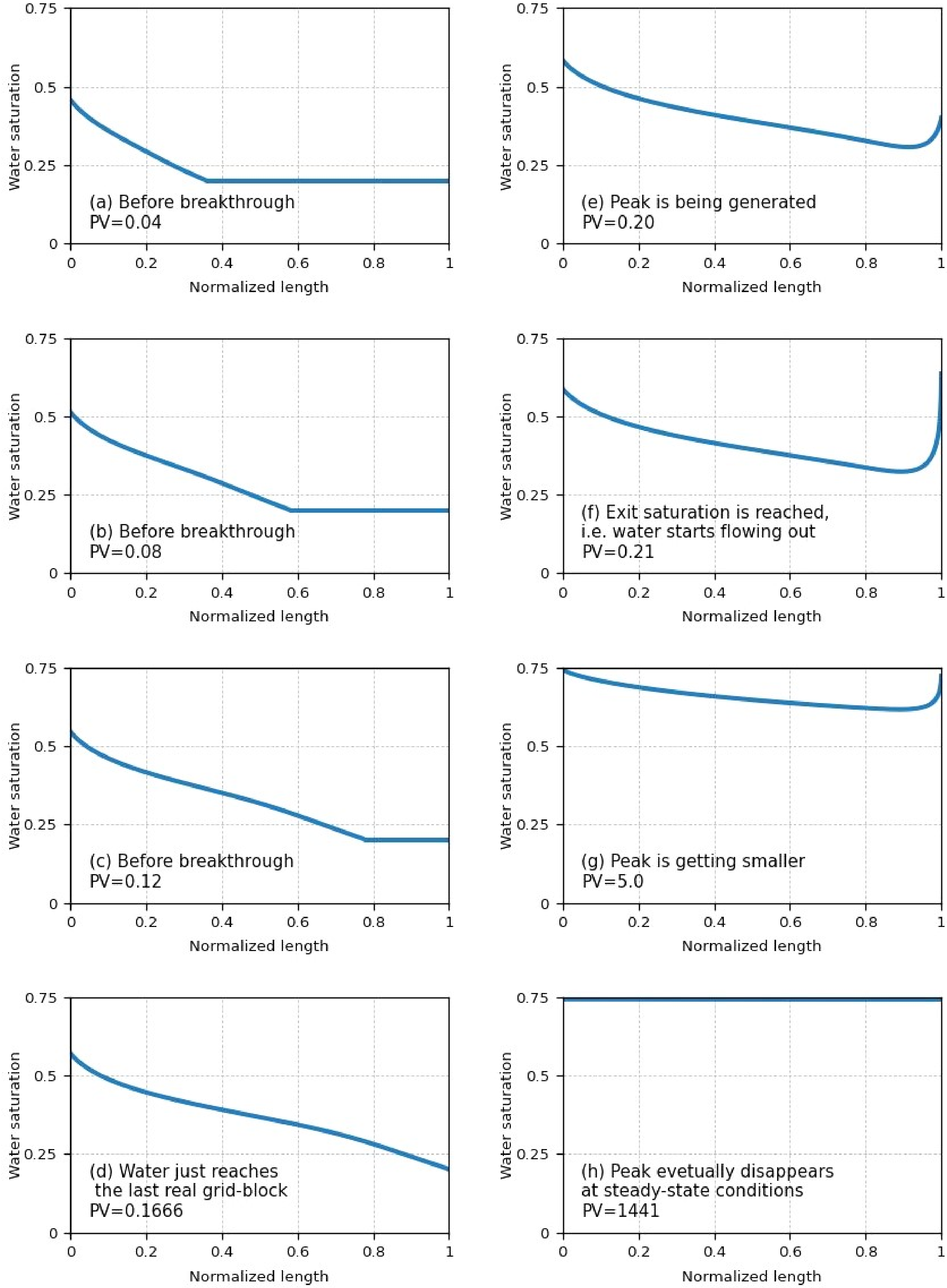

Fig. 13. Water saturation profiles during the displacement process in a water-wet system.

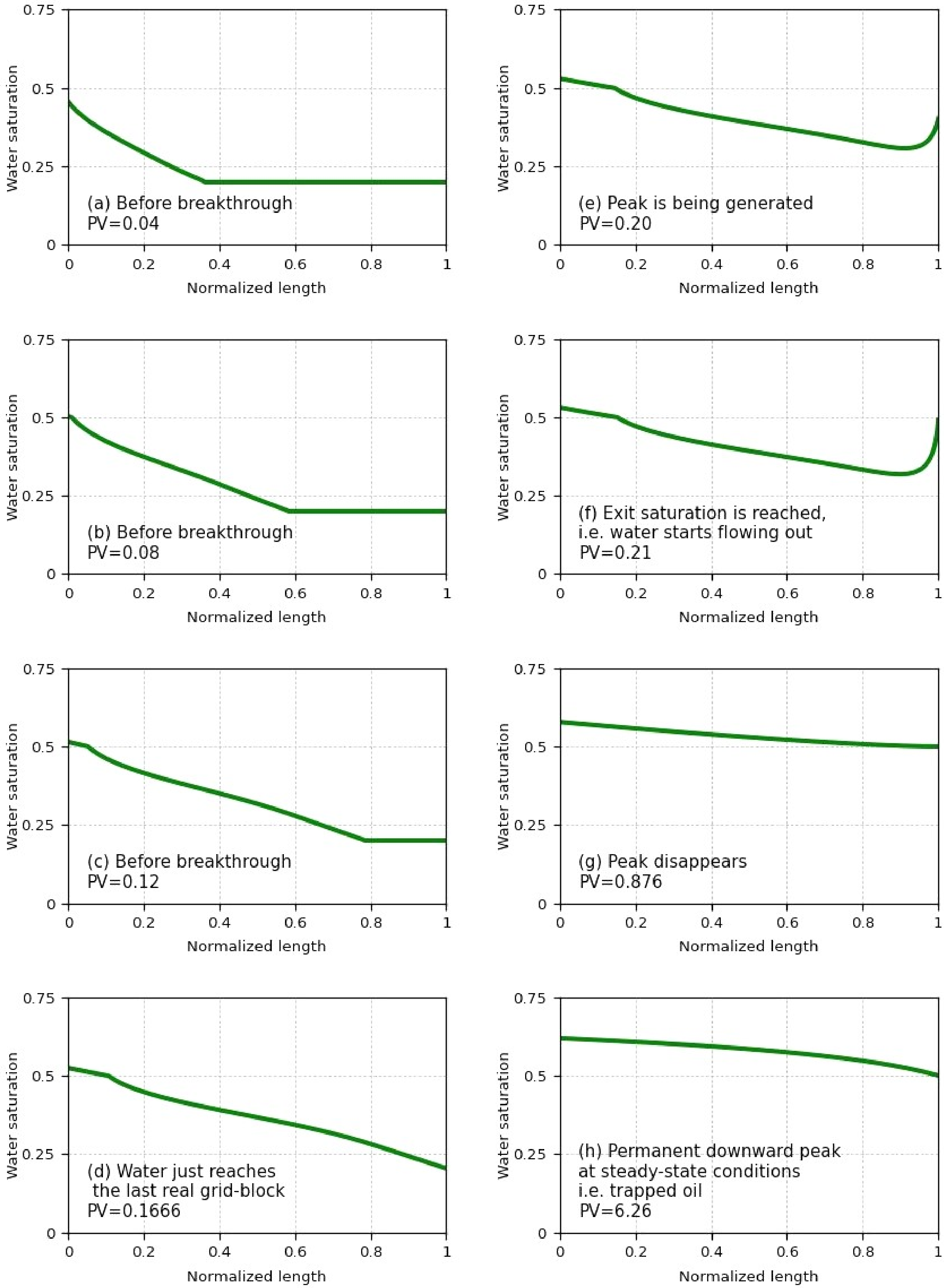

Fig. 14. Water saturation profiles during the displacement process in a mixed-wet system.

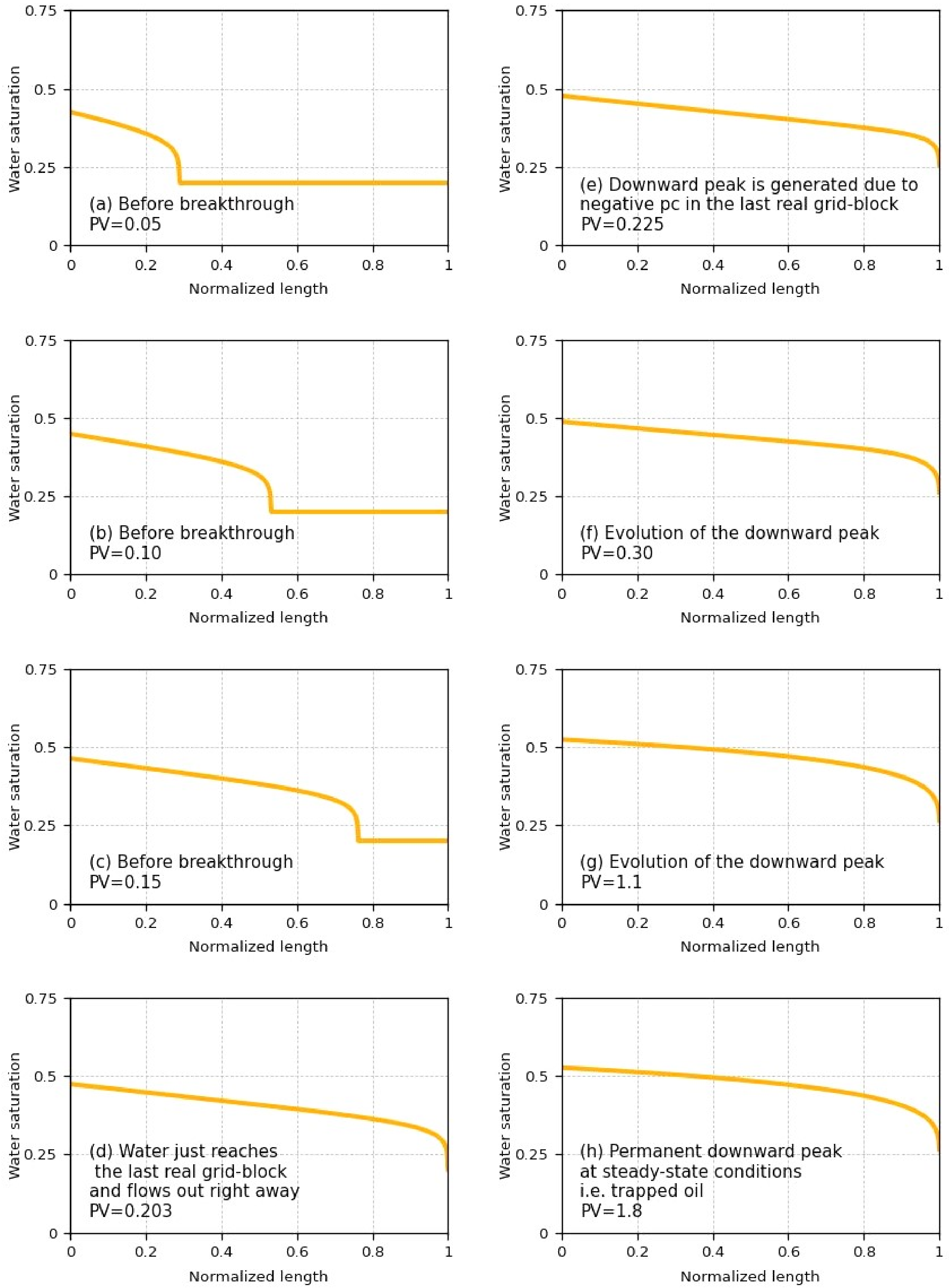

Fig. 15. Water saturation profiles during the displacement process in an oil-wet system.

Table 1 and Eq. (1), with $k = 132.95$ mD and $q = 184.90$ cc/hr.

1) **Before breakthrough:** The plots "a, b, and c" in Figs. 13, 14 and 15 show the progress of the "fronts" at different times before breakthrough for water-, mixed- and oil-wet cases, respectively. The front, in water- and mixed-wet systems, is clearly very spread out due to the dominant effect of capillary pressure. The underlying "Buckley-Leverett" shock fronts are barely evident in these profiles. Note that there is a small "kink" in the water saturation profiles of the mixed-wet case in Fig. 14. This kink exactly at $S_w = 0.5$ is caused by the chosen mixed-wet capillary pressure function which is continuous between the water-wet ($S_w \leq 0.5$) and oil-wet ($S_w > 0.5$) sections, but the first derivative, $\mathrm{d}p_c/\mathrm{d}S_w$, is not continuous. The front for the oil-wet case is quite sharp since $\mathrm{d}p_c/\mathrm{d}S_w \approx 0$ at low water saturation values (see Fig. 2), hence the diffusion is low in this region. Water then reaches the last real grid-block (shown in plot "d" in Figs. 13, 14 and 15), after which the effect of capillary discontinuity is observed.
2) **Peak generation:** If there were no capillary pressure discontinuity at the outlet, water would flow out in just one timestep after water reaches the last real grid-block, because $k_{rw} > 0$ when $S_w > S_{wc}$. However, when water reaches the last real grid-block, it is held back in water- and mixed-wet systems (shown in several of the plots in Figs. 13 and 14) until exit saturation is reached. No such peak is observed for the oil-wet case, hence $S_{w,exit} = S_{wc}$ (in Fig. 15(d)) as explained above.
3) **Exit saturation:** Explained in detail above and seen in Figs. 13(f) and 14(f).
4) **Peak evolution and late-time behaviour**: In water-wet cores, after breakthrough, water saturation keeps rising at the end of the system as the displacement continues with time (in Fig. 13(g)), consequently capillary pressure decreases there with time (rock becomes more saturated and continues to lose its tendency to prevent water from flowing out). Therefore, the negative capillary pressure gradient ($\nabla p_c = (p_{cb} - p_{c,N_x,1})/0.5\Delta x = (0 - p_{c,N_x,1})/0.5\Delta x$) that holds water back in the system reduces, hence water feels less resistance to flow out and the CEE diminishes with time. This process continues until water saturation in the last real grid-block (and the whole system) reaches $1 - S_{or}$ and all oil is displaced out (at steady-state conditions), however this may take a *very* long time. At steady-state conditions, negative capillary pressure gradient becomes zero and disappears. Note plot in Fig. 13(h) where 1,441 PV of water is required to reach a recovery factor of 0.999.

In Mixed-wet cores, when water saturation exceeds $S_w = 0.5$, the value of capillary pressure becomes more negative (see the green curve in Fig. 2). Increasing the water saturation in the last real grid-block as displacement continues with time increases the capillary pressure gradient that favours water flow, hence limits oil flow (as it is an incompressible displacement process with fixed total flowrate) by reducing oil-phase pressure gradient. For this reason, oil flows out at a slower rate, therefore water saturation in the last real grid-block increases at a slower rate too (i.e., oil does not flow out to leave space for water to occupy). Oil-phase pressure gradient continues to reduce until it becomes zero. At this point which marks steady-state conditions, only water flows out, and its saturation becomes "pinned" because no more oil will flow out of the system. This region with depleted water and stagnant oil near the outlet with zero oil-phase pressure gradient is called the CEE region. In some cases, the CEE region can take up the whole length of the system. The final profile in the mixed-wet system is shown in Fig. 14(h). This is the final oil recovery that is possible *in principle* at this flowrate. Oil recovery could be increased if the flowrate was increased. Note that after exit saturation is reached in mixed-wet systems, water saturation at the outlet is $S_w = 0.5$ (asymptotically) for the rest of the displacement process.

In ***oil-wet cores***, when water enters the last real grid-block, capillary pressure becomes negative (the orange curve in Fig. 2), and this creates a positive capillary pressure gradient at the end of the system which favours water flow and limits oil flow by reducing oil-phase pressure gradient. This causes a "downward peak" just like the long-time mixed-wet case (Fig. 15). Like the mixed-wet case, oil-phase pressure gradient keeps decreasing as displacement continues, and reaches zero eventually, for which oil gets trapped, and water saturation becomes pinned in the system at a certain value. Again, the same CEE region (with depleted water and stagnant oil) will exist here in which oil is trapped permanently, with no more production at this flowrate. Note that after two-phase flow is established, water saturation at the outlet is $S_w = S_{wc}$ (asymptotically) for the rest of the displacement process.

Note that in all wetting systems, a steady-state condition is achieved sooner when oil viscosity is lower due to higher mobility. Two further important points for the mixed- and oil-wet cases are as follows:

- The final phase saturation profile along the system depends only on the water viscosity, however it sounds counter-intuitive that the final steady-state saturation does not depend on the oil viscosity.
- The steady-state phase saturation profile can be calculated (a priori) semi-analytically which agrees perfectly identical to the results of the formulation introduced here when it is run long enough to reach steady-state conditions (see below).

7. Semi-analytical calculation of the final (steady-state) saturation profiles

Another consequence of taking a discretized approach to the problem of the CEE is that water saturation profiles at steady-state conditions can be calculated semi-analytically. The steady-state conditions of the system can be found numerically by running the transient code (the formulation introduced above) sufficiently long enough that the water saturation profile no longer changes. Three semi-analytical methods are presented here to quickly obtain the water saturation profile at steady-state conditions. Note that these methods are only for mixed- and oil-wet systems, since in water-wet systems water saturation at steady-state conditions is $S_w = 1 - S_{or}$ at all points (although this may take a very long time - in PV).

7.1 Integral method for calculating the steady-state saturation profile

Water volumetric flowrate is known to be $q_w = -kA\lambda_w(\nabla p_o - \nabla p_c)$. As explained above, at steady-state conditions, oil-phase pressure gradient is zero along the CEE region, i.e., $\nabla p_o = 0$. Therefore, the water flowrate in the CEE region is $q_w = kA\lambda_w \nabla p_c$, which means $\nabla p_c = \partial p_c/\partial x = \partial p_c/\partial S_w \, \partial S_w/\partial x = q_w/kA\lambda_w$. This leads to:

$$\int_{x_a}^{L} \mathrm{d}x = L - x_a = \int_{S_{wa}}^{0.5} \frac{kA\dfrac{\mathrm{d}p_c}{\mathrm{d}S_w}}{\dfrac{q_w}{\lambda_w}} \mathrm{d}S_w \tag{7}$$

where x_a is the location (distance from the inlet) of any arbitrary value of water saturation, say S_{wa}, that is in the range $0.5 < S_{wa} < 1 - S_{or}$. Therefore, x_a would be equal to L when $S_{wa} = 0.5$. For any value of S_{wa} this integral gives a unique value for x_a which can be used to plot the final water saturation profile. Huang and Honarpour (1996) presented an integral method suitable for oil/water co-injection problems. However, in this work only water is injected into an oil-filled system. Also, the calculation above is based on the fact that oil-phase pressure gradient is zero in the CEE region at the steady-state conditions.

7.2 Pressure-based calculation for the steady-state saturation profile

Again, using the fact that oil-phase pressure gradient is zero ($\nabla p_o = 0$) along the CEE region at steady-state conditions, the water flow from the last real grid-block is as follows:

$$q_w = q_{inj} = kA\lambda_{w,N_x,1} \frac{0 - p_{c,N_x,1}}{0.5\Delta x} \tag{8}$$

Eq. (8) can be rearranged to the following form:

$$F(S_w) = kA\lambda_{w,N_x,1} \frac{0 - p_{c,N_x,1}}{0.5\Delta x} - q_{inj} = 0 \tag{9}$$

Any non-linear solver, such as the Bisection or Newton-Raphson method, can be used to find the water saturation in the last real grid-block at steady-state conditions, by solving the above non-linear equation. The same approach can be used to obtain the water saturation in all other grid-blocks working sequentially back from the final block all the way to the first (inlet) grid-block, as follows:

$$kA\lambda_{w,i,1} \frac{p_{c,i+1,1} - p_{c,i,1}}{\Delta x} - q_{inj} = 0 \tag{10}$$

An important calculation note is that, when Eq. (10) has a solution greater than $S_w > 1 - S_{or}$, then at this point in the system the CEE region starts, i.e., a region unaffected by the CEE is reached. The unaffected and the CEE regions are shown in Figs. 16 and 17.

Eq. (8) helps us answer the following question: At what water injection rate into the mixed-wet system, the CEE region will be completely removed, and no oil would be permanently trapped in the system? Higher injection rate reduces the length of the CEE region and improves oil recovery, but from Eq. (8), no matter how high the injection rate is, there will be a distance from the outlet that satisfies the equation. Therefore, the CEE region cannot be removed completely (theoretically), and some oil will always be trapped in the system. For more detailed explanation, see Chapter 7 in Goodarzian (2021).

7.3 Saturation-based calculation from convection-dispersion formulation

This final approach to calculating the steady-state saturation profile along the system comes from the convection/-capillary dispersion formulation of the problem (Stephen et al., 2001; Goodarzian, 2021). Flow of water from the last grid-block through the system outlet is obtained using the following equation:

$$q_w = q_{inj} = q_{inj} f_{wv,N_x,1} - A\phi g(S_{w,N_x,1}) \frac{p_{cb} - p_{c,N_x,1}}{0.5\Delta x} \tag{11}$$

where $g(S_w) = (-k/\phi)/(1/\lambda_o + 1/\lambda_w)$ is the capillary diffusivity term that is inherently negative and $p_{cb} = 0$. Therefore, before water saturation in the last grid-block reaches $S_w = 0.5$ (in this study), the second term on the RHS in Eq. (11) is negative (since capillary pressure is positive for $S_w < 0.5$), thus holding water back which creates an upward peak in the water saturation profile. After water saturation goes above $S_w = 0.5$, then the mixed-wet capillary pressure becomes negative and the second term on the RHS becomes positive. Water outflow is thus enhanced, which limits oil outflow via reducing the oil-phase pressure gradient until it becomes zero at steady-state conditions. Eq. (11) can be solved by numerical methods:

$$F(S_w) = q_{inj} f_{wv,N_x,1} - A\phi g(S_{w,N_x,1}) \frac{p_{cb} - p_{c,N_x,1}}{0.5\Delta x} - q_{inj} = 0 \tag{12}$$

For other grid-blocks, the following equation is used:

$$q_w = q_{inj} = q_{inj} f_{wv,i,1} - A\phi g(S_{w,i,1}) \frac{p_{c,i+1,1} - p_{c,i,1}}{\Delta x} \tag{13}$$

In Fig. 16, steady-state water saturation profiles obtained from 4 methods in a mixed-wet system are shown to be identical. This confirms that all of these methods capture the physics of the problem correctly; explained in full detail in Goodarzian (2021). For this simulation example, the same relative permeability and capillary pressure functions are used again. Also, $q_{inj} = 43.461$ cc/min and $\mu_w = 0.5$ cp and $\mu_o = any\ value$ are used. Note that oil viscosity has no effect on the steady-state water saturation profile. In Fig. 17, the same simulation is run for an oil-wet system (with the oil-wet capillary pressure function in Eq. (1) and Fig. 2). Again, steady-state water saturation profiles obtained from 4 methods are shown to be identical. This confirms that the proposed formulation gives exact results (to machine accuracy) when it is run sufficiently long to reach effectively the steady-state conditions.

8. Summary and conclusions

The IMPES and 1D convection-capillary dispersion formulations of the two-phase flow equations are modified to capture

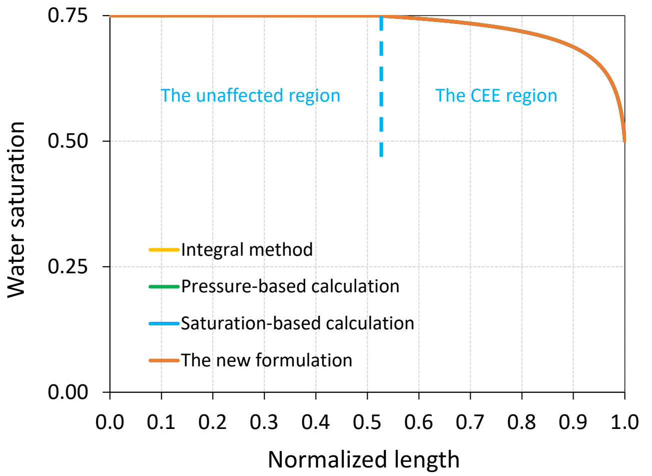

Fig. 16. S_w profile at steady-state conditions obtained from 4 methods for the mixed-wet system.

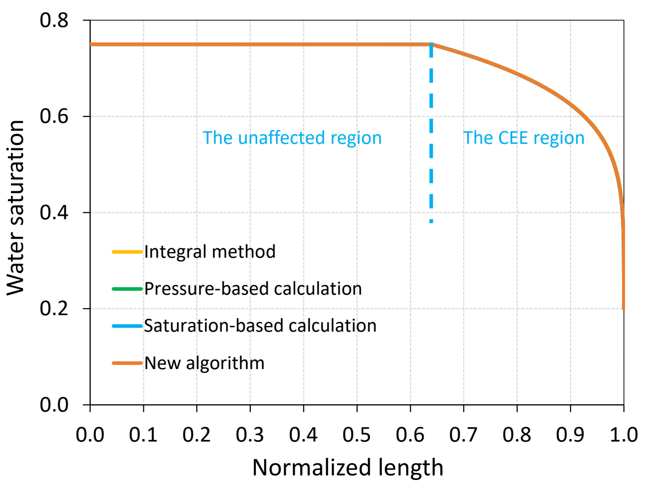

Fig. 17. S_w profile at steady-state conditions obtained from 4 methods for the oil-wet system.

the point of capillary pressure discontinuity at the end of 1D systems in a two-phase waterflood process, i.e., to model the CEE. This modification guarantees mass conservation which is not the case when the conventional IMPES formulation is used for this problem. It is shown that dummy grid-blocks are not necessary to solve this problem as they do not add any physics to calculations. Likewise, LGR does not help to solve the CEE effect for the same reason. Correct equations and boundary conditions are required to solve this problem exactly, which are described in this work. It is shown that commercial simulators do not deal with the CEE problem rigorously, leading to small errors for the saturation values and mass balance calculations. The reason for this error was diagnosed by implementing the (incorrect) "fix-up method" which these commercial codes use and finding that their exact values (to several decimal places) can be reproduced.

From the correct treatment of the CEE boundary condition, then a simple implicit equation is developed to calculate the value of "exit saturation", i.e., the value of water saturation in the last "real" grid-block at which water just flows out of the system, after building up for a while. An exit saturation with $S_{w,exit} > S_{wc}$ develops for water- or mixed-wet systems (always less than the value at which capillary pressure is zero), while there is no water build-up in purely oil-wet systems. Exit saturation is lower at higher flowrates, higher oil viscosity and lower absolute permeability because of a stronger viscous pressure gradient in the system. It is also shown that water viscosity has no effect on the value of exit saturation.

A central feature of the water-wet system is that no matter how severe the CEE is, the long-term flooding behaviour is that all the movable oil is ultimately produced, and the CEE cannot persist "forever" even at a very slow flowrate. In mixed- and oil-wet systems, the CEE persists "forever" at any flowrate as a positive capillary pressure gradient develops at the end of the system, which favours water flow and limits oil flow by reducing oil-phase pressure gradient which ultimately drops to zero at steady-state conditions. This causes oil to be trapped in the system "forever" because of zero oil-phase pressure gradient, while still being potentially mobile (for $k_{ro} > 0$). Oil recovery could only be increased by increasing the flowrate in these systems. Also, oil viscosity has no effect on the water saturation profile at steady-state conditions in mixed- and oil-wet systems, but steady-state conditions are reached later when oil is more viscous. Three semi-analytic methods are presented to calculate the steady-state saturation profile in mixed- and oil-wet systems which is shown to agree exactly with the numerically calculated final steady-state profile.

Conflict of interest

The authors declare no competing interest.

References

Aziz, K., Settari, A. Petroleum Reservoir Simulation. London, UK, Applied Science Publishers, 1979.

Goodarzian, S. Modelling of the capillary end effect in systems of variable wettability. Edinburgh, Heriot-Watt University, 2021.

Goodarzian, S., Sorbie, K. A Rigorous Method for Special Core Analysis SCAL Data Correction in the Presence of Capillary End Effects. Amsterdam, Netherlands, SPE Europec featured at 82nd EAGE Conference and Exhibition, 2020.

Goodarzian, S., Sorbie, K. Correct relative permeability data from steady-state experiments for capillary end effects. Journal of Geoenergy Science and Engineering, 2023, 224: 211626.

Gupta, R., Maloney, D. R. Intercept method-a novel technique to correct steady-state relative permeability data for capillary end-effects. Paper SPE 171797 Presented at the Abu Dhabi International Petroleum Exhibition and Conference, Abu Dhabi, UAE, 10-13 November, 2014.

Hadley, G. F., Handy, L. L. A Theoretical and experimental study of the steady state capillary end effect. Paper SPE 707-G Presented at the Fall Meeting of the Petroleum

Branch of AIME, Los Angeles, California, 14-17 October 1956.

Huang, D. D., Honarpour, M. M. Capillary end effects in coreflood calculations. Paper 9634 Presented at the 1996 International Symposium of the Society of Core Analysis, Montpellier, France, 8-10 September, 1996.

Kyte, J. R., Rapoport, L. A. Linear waterflood behaviour and end effects in water-wet porous media. Journal of Petroleum Technology, 1958, 10(10): 47-50.

Leverett, M. C. Capillary behaviour in porous solids. Transactions of the AIME, 1941, 142(1): 152–169.

Masalmeh, S. K. Impact of capillary forces on residual oil saturation and flooding experiments for mixed to oil-wet carbonate reservoirs. Paper SCA2012-11 Presented at the International Symposium of the Society of Core Analysts, Aberdeen, Scotland, UK, 27-30 August, 2012.

Nazari, R., Jamiolahmadi, M. Steady-state relative permeability measurements of tight and shale rocks considering capillary end effect. Transport in Porous Media, 2019, 128: 75-96.

Peaceman, D. W. Fundamentals of Numerical Reservoir Simulation. Developments in Petroleum Science, Elsevier, Houston, Texas, USA, 1977.

Pinder, G. F., Gray, W. G. Essentials of Multiphase Transport in Porous Media. New York, USA, Wiley, 2008.

Richardson, J. G., Kerver, J. K., Hafford, J. A., et al. Laboratory determination of relative permeability. Journal of Petroleum Technology, 1952, 4(8): 187-196.

Stephen, K. D., Pickup, G. E., Sorbie, K. S. The local analysis of changing force balances in immiscible incompressible two-phase flow. Transport in Porous Media, 2001, 45: 63-88.

van Duijn, C. J., de Neef, M. J. Similarity solution for capillary redistribution of two phases in porous medium with a single discontinuity. Advances in Water Resources, 1998, 21(6): 451-461.

Virnovsky, G. A., Skjaeveland, S. M., Surdal, J., et al. Steady-state relative permeability measurements corrected for capillary effects. Paper SPE 30541 Presented at the SPE Annual Technical Conference and Exhibition, Dallas, Texas, 22-25 October, 1995.

Virnovsky, G. A., Vatne, K. O., Skjaeveland, S. M., et al. Implementation of multirate technique to measure relative permeabilities accounting. Paper SPE 49321 Presented at the SPE Annual Technical Conference and Exhibition, New Orleans, Louisiana, 27-30 September, 1998.

Appendix.

The conventional IMPES formulation works only when all grid-blocks follow the same capillary pressure function. In the CEE problem, at the outlet, capillary pressure suddenly becomes zero, therefore boundary point MUST be treated on its own with its unique property ($p_c = 0$). To honour this condition, an extra equation for the boundary is required which contains a new variable p_{ob} (the oil-phase pressure at the outlet), which is updated in each timestep. In addition, two existing equations for the last real grid-block and the first dummy grid-block must be modified.

1. Modification of the IMPES method in the presence of 200 dummy grid-blocks

Equation for the outlet prescribing oil flux continuity

Water outflow at any time is $q_{w,out} = 2a\lambda_{w,N_x,1}\left(p^{n+1}_{o,N_x,1} - p^{n+1}_{ob} + p_{cb} - p^{n}_{c,N_x,1}\right)$, as in Eq. (2). If $q_{w,out} \leq 0$, only oil leaves grid-block $i = N_x$ which enters grid-block $i = N_x + 1$, therefore,

$$a\lambda_{o,N_x,1}\frac{p^{n+1}_{o,N_x,1} - p^{n+1}_{ob}}{0.5} = a\lambda_{o,N_x,1}\frac{p^{n+1}_{ob} - p^{n+1}_{o,N_x+1,1}}{0.5} \tag{A1}$$

where $a = k\Delta y\Delta z/\Delta x$. Upstream weighting must be applied because what goes into grid-block $i = N_x + 1$ is determined by the phase mobility in grid-block $i = N_x$.

Modification of equations for grid-block $i = N_x$

If $q_{w,out} \leq 0$, oil and (possibly) water can enter this grid-block but only oil leaves it,

$$a\lambda_{t,N_x-1,1}\left(p^{n+1}_{o,N_x-1,1} - p^{n+1}_{o,N_x,1}\right) + a\lambda_{w,N_x-1,1}\left(p^{n}_{c,N_x,1} - p^{n}_{c,N_x-1,1}\right) = a\lambda_{o,N_x,1}\frac{p^{n+1}_{o,N_x,1} - p^{n+1}_{ob}}{0.5} \tag{A2}$$

Water saturation in this grid-block is calculated by the following equation, in which $q_{w,out}$ is **reset to zero automatically in the code** since it cannot be negative.

$$S^{n+1}_{w,N_x,1} = S^{n}_{w,N_x,1} + \frac{\Delta t}{\Delta x\Delta y\Delta z\phi}\left\{a\lambda_{w,N_x-1,1}\left(p^{n+1}_{o,N_x-1,1} - p^{n+1}_{o,N_x,1} + p^{n}_{c,N_x,1} - p^{n}_{c,N_x-1,1}\right) - q_{w,out}\right\} \tag{A3}$$

Modification of equations for grid-block $i = N_x + 1$

If $q_{w,out} \leq 0$, only oil flows in and out of this grid-block and enters the next dummy grid-block,

$$a\lambda_{o,N_x,1}\frac{p^{n+1}_{ob} - p^{n+1}_{o,N_x+1,1}}{0.5} = a\lambda_{t,N_x+1,1}\left(p^{n+1}_{o,N_x+1,1} - p^{n+1}_{o,N_x+2,1}\right) \tag{A4}$$

In this case $\lambda_{t,N_x+1,1} = \lambda_{o,N_x+1,1}$. Water saturation in this grid-block does not change, as shown below,

$$S^{n+1}_{w,N_x+1,1} = S^{n}_{w,N_x+1,1} + \frac{\Delta t}{\Delta x\Delta y\Delta z\phi}\{zero\} = S^{n}_{w,N_x,1} \tag{A5}$$

This "zero" is because no water enters or leaves this grid-block, hence saturation remains constant.

Equation for the outlet prescribing total mass flux continuity

For an incompressible displacement, total flowrate is constant at all points. If $q_{w,out} > 0$ (or when $S_{w,N_x,1} \geq S_{w,exit}$), both oil and water leave the last real grid-block which enter the first dummy grid-block,

$$a\lambda_{t,N_x,1}\frac{p^{n+1}_{o,N_x,1} - p^{n+1}_{ob}}{0.5} + a\lambda_{w,N_x,1}\frac{p_{cb} - p^{n}_{c,N_x,1}}{0.5} = a\lambda_{t,N_x,1}\frac{p^{n+1}_{ob} - p^{n+1}_{o,N_x+1.1}}{0.5} + a\lambda_{w,N_x,1}\frac{p^{n}_{c,N_x+1.1} - p_{cb}}{0.5} \tag{A6}$$

Modification of equations for grid-block $i = N_x$

If $q_{w,out} > 0$, there is a two-phase flow of oil and water into and out of this grid-block, therefore,

$$a\lambda_{t,N_x-1,1}\left(p^{n+1}_{o,N_x-1,1} - p^{n+1}_{o,N_x,1}\right) + a\lambda_{w,N_x-1,1}\left(p^{n}_{c,N_x,1} - p^{n}_{c,N_x-1,1}\right) = a\lambda_{t,N_x,1}\frac{p^{n+1}_{o,N_x,1} - p^{n+1}_{ob}}{0.5} + a\lambda_{w,N_x,1}\frac{p_{cb} - p^{n}_{c,N_x,1}}{0.5} \tag{A7}$$

Water saturation in this grid-block is calculated by the following expression, knowing that outgoing water leaving this grid-block is the water outflow term, i.e., $q_{w,out} = 2a\lambda_{w,N_x,1}(p^{n+1}_{o,N_x,1} - p^{n+1}_{ob} + p_{cb} - p^{n}_{c,N_x,1})$.

$$S^{n+1}_{w,N_x,1} = S^{n}_{w,N_x,1} + \frac{\Delta t}{\Delta x\Delta y\Delta z\phi}\{a\lambda_{w,N_x-1,1}(p^{n+1}_{o,N_x-1,1} - p^{n+1}_{o,N_x,1} + p^{n}_{c,N_x,1} - p^{n}_{c,N_x-1,1}) - q_{w,out}\} \tag{A8}$$

Modification of equations for grid-block $i = N_x + 1$

If $q_{w,out} > 0$, both oil and water enter and leave this grid-block, then,

$$a\lambda_{t,N_x,1}\frac{(p^{n+1}_{ob} - p^{n+1}_{o,N_x+1,1})}{0.5} + a\lambda_{w,N_x,1}\frac{(p^{n}_{c,N_x+1,1} - p_{cb})}{0.5} = a\lambda_{t,N_x+1,1}(p^{n+1}_{o,N_x+1,1} - p^{n+1}_{o,N_x+2,1}) + a\lambda_{w,N_x+1,1}\left(p^{n}_{c,N_x+2,1} - p^{n}_{c,N_x+1,1}\right) \tag{A9}$$

Water saturation in this grid-block is calculated as follows.

$$S_{w,N_x+1,1}^{n+1} = S_{w,N_x+1,1}^{n} + \frac{\Delta t}{\Delta x \Delta y \Delta z \phi} \left\{ q_{w,out} - a\lambda_{w,N_x+1,1} \left(p_{o,N_x+1,1}^{n+1} - p_{o,N_x+2,1}^{n+1} + p_{c,N_x+2,1}^{n} - p_{c,N_x+1,1}^{n} \right) \right\} \quad \text{(A10)}$$

2. The case with one dummy grid-block

The methodology is the same for only one dummy grid-block. The equations for the boundary and for the last real grid-block will be the same in each continuity formulation, as shown above. Only the equation for the first dummy grid-block needs to be modified, in which the well is now located, therefore the fluid leaving this dummy grid-block is the fluid that is produced, as shown in Fig. A1.

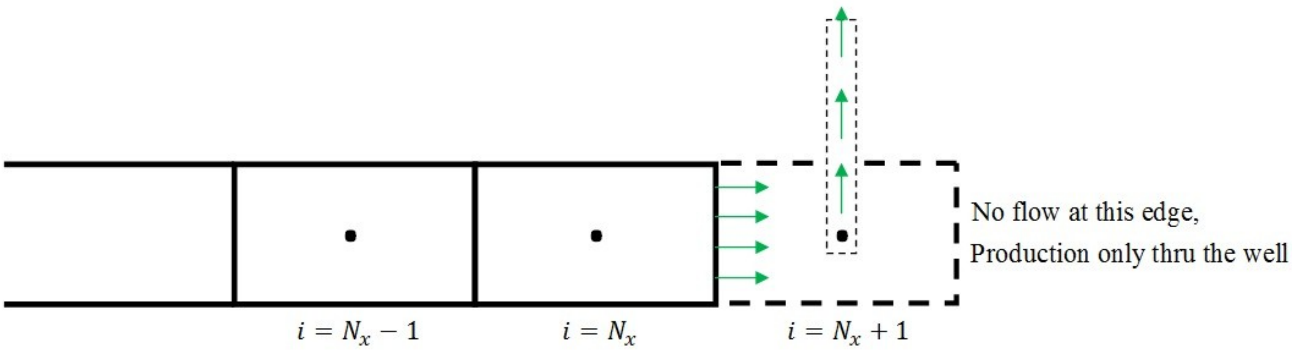

Fig. A1. Arrangement of grid-blocks when only one dummy grid-block is employed.

Modification of equations for grid-block $i = N_x + 1$ prescribing oil flux continuity

If $q_{w,out} \leq 0$, only oil leaves grid-block $i = N_x$ which enters grid-block$i = N_x + 1$.

$$a\lambda_{o,N_x,1} \frac{(p_{ob}^{n+1} - p_{o,N_x+1,1}^{n+1})}{0.5} = W_{index}\lambda_{t,N_x+1,1} \left(p_{o,N_x+1,1}^{n+1} - p_{well} \right) \quad \text{(A11)}$$

where $a = k\Delta y \Delta z / \Delta x$, $W_{index} = (2\pi) k\Delta z / \ln(r_b/r_w)$, and $r_b = \sqrt{\Delta x \Delta y / e\pi}$. In this case $\lambda_{t,N_x+1,1} = \lambda_{o,N_x+1,1}$. Water saturation stays the same in this dummy grid-block because of no water inflow and outflow.

Modification of equations for grid-block $i = N_x + 1$ prescribing total mass flux continuity

If $q_{w,out} > 0$, both oil and water enter and leave this grid-block, then,

$$a\lambda_{t,N_x,1} \frac{(p_{ob}^{n+1} - p_{o,N_x+1,1}^{n+1})}{0.5} + a\lambda_{w,N_x,1} \frac{(p_{c,N_x+1,1}^{n} - p_{cb})}{0.5} = W_{index}\lambda_{t,N_x+1,1} \left(p_{o,N_x+1,1}^{n+1} - p_{well} \right) \quad \text{(A12)}$$

Incoming water to this grid-block is water outflow. Then, water saturation in this grid-block is as follows,

$$S_{w,N_x+1,1}^{n+1} = S_{w,N_x+1,1}^{n} + \frac{\Delta t}{\Delta x \Delta y \Delta z \phi} \left\{ q_{w,out} - W_{index}\lambda_{w,N_x+1,1} \left(p_{o,N_x+1,1}^{n+1} - p_{well} \right) \right\} \quad \text{(A13)}$$

Now there are 1,000 equations for 1,000 real grid-blocks, one equation for the boundary, and one equation for one dummy grid-block, therefore 1002 equations compared to 1201 equations when there were 200 dummy grid-blocks which reduces the simulation time significantly.

3. The case with no dummy grid-blocks

Capillary pressure at the outlet is zero and oil and water have equal pressures, say 4,500 psi (as in Fig. A2). It is now only needed to modify the equation for grid-block $i = N_x$ as there is no dummy grid-block.

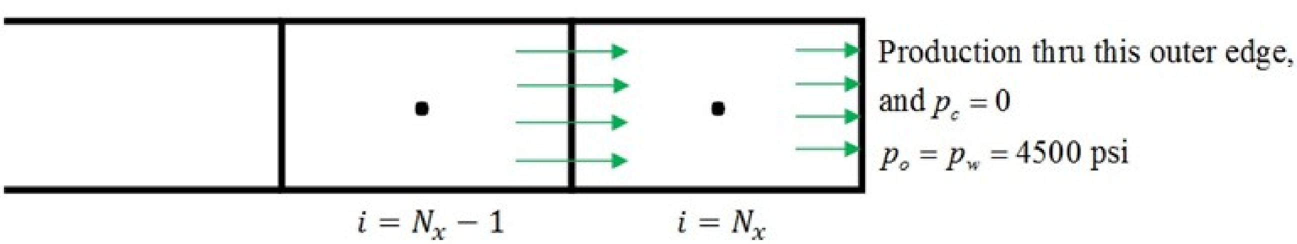

Fig. A2. Arrangement of grid-blocks when no dummy grid-block is employed.

Modification of equations for grid-block $i = N_x$ prescribing oil flux continuity

If $q_{w,out} \leq 0$, only oil leaves grid-block $i = N_x$ and is produced through the outlet.

$$a\lambda_{t,N_x-1,1}(p^{n+1}_{o,N_x-1,1} - p^{n+1}_{o,N_x,1}) + a\lambda_{w,N_x-1,1}(p^{n}_{c,N_x,1} - p^{n}_{c,N_x-1,1}) = a\lambda_{o,N_x,1}\frac{(p^{n+1}_{o,N_x,1} - p_{ob})}{0.5} \tag{A14}$$

Water may be flowing into this grid-block, but no water leaves this grid-block due to capillary hold-up. Water saturation is obtained by the following equation,

$$S^{n+1}_{w,N_x,1} = S^{n}_{w,N_x,1} + \frac{\Delta t}{\Delta x\Delta y\Delta z\phi}\left\{a\lambda_{w,N_x-1,1}\left(p^{n+1}_{o,N_x-1,1} - p^{n+1}_{o,N_x,1} + p^{n}_{c,N_x,1} - p^{n}_{c,N_x-1,1} - zero\right)\right\} \tag{A15}$$

Modification of equations for grid-block $i = N_x$ prescribing total mass flux continuity

If $q_{w,out} > 0$, both oil and water enter and leave this grid-block, then,

$$a\lambda_{t,N_x-1,1}(p^{n+1}_{o,N_x-1,1} - p^{n+1}_{o,N_x,1}) + a\lambda_{w,N_x-1,1}(p^{n}_{c,N_x,1} - p^{n}_{c,N_x-1,1}) = a\lambda_{t,N_x,1}\frac{(p^{n+1}_{o,N_x,1} - p_{ob})}{0.5} + a\lambda_{w,N_x,1}\frac{(p_{cb} - p^{n}_{c,N_x,1})}{0.5} \tag{A16}$$

Note that p_{ob} will remain fixed during the whole displacement process. Now there are both incoming water and outflowing water, therefore water saturation is calculated using the following equation,

$$S^{n+1}_{w,N_x,1} = S^{n}_{w,N_x,1} + \frac{\Delta t}{\Delta x\Delta y\Delta z\phi}\left\{a\lambda_{w,N_x-1,1}\left(p^{n+1}_{o,N_x-1,1} - p^{n+1}_{o,N_x,1} + p^{n}_{c,N_x,1} - p^{n}_{c,N_x-1,1}\right) - q_{w,out}\right\} \tag{A17}$$

In this method there are only 1000 equations for 1000 grid-blocks, hence an even faster formulation.

4. Modified 1D convection-diffusion formulation-explicit scheme

The various arguments and developments in the main text of the paper are based on IMPES formulation, and its discretization. Here, a convection-capillary dispersion form of the two-phase transport equation is used to solve the CEE problem, without employing dummy grid-blocks. The differential equation representing the evolution of water saturation with respect to time and location is given by Eq. (A18),

$$\frac{\partial S_w}{\partial t} = -\frac{q_t}{A\phi}\frac{\partial f_{wv}}{\partial x} + \frac{\partial}{\partial x}\left(-\frac{k}{\phi}\frac{\lambda_o\lambda_w}{\lambda_o + \lambda_w}\nabla p_c\right) \tag{A18}$$

This equation can be solved numerically by taking an explicit scheme, with no need to calculate pressure value in grid-blocks. The correct boundary condition (as explained in the text) is implemented to properly represent the outlet point with zero capillary pressure. For this formulation, the equation for the last real grid-block is as follows,

$$\frac{S^{n+1}_{w,N_x,1} - S^{n}_{w,N_x,1}}{\Delta t} = \frac{q_t}{A\phi}\frac{f_{wv,N_x-1,1}}{\Delta x} - \frac{q_t}{A\phi}\frac{f_{wv,N_x,1}}{\Delta x} + \frac{-A\phi g\,(S_w)^n_{N_x-1,1}\dfrac{p^{n}_{c,N_x,1} - p^{n}_{c,N_x-1,1}}{\Delta x}}{A\Delta x\phi} - \frac{-A\phi g\,(S_w)^n_{N_x-1,1}\dfrac{0 - p^{n}_{c,N_x,1}}{0.5\Delta x}}{A\Delta x\phi} \tag{A19}$$

where $g(S_w) = -(k/\Phi)(\lambda_o\lambda_w/(\lambda_o + \lambda_w))$ is inherently negative. In Eq. (A19), the first term on the RHS denotes amount of water entering the last grid-block and the second term denotes amount of water leaving this grid-block, due to advection and capillarity. The third term indicates amount of water entering the last grid-block in each timestep under capillary action only and the fourth term denotes amount of water withheld by capillary action in water-wet systems or discharged in oil-wet systems (all terms shown in Fig. A3).

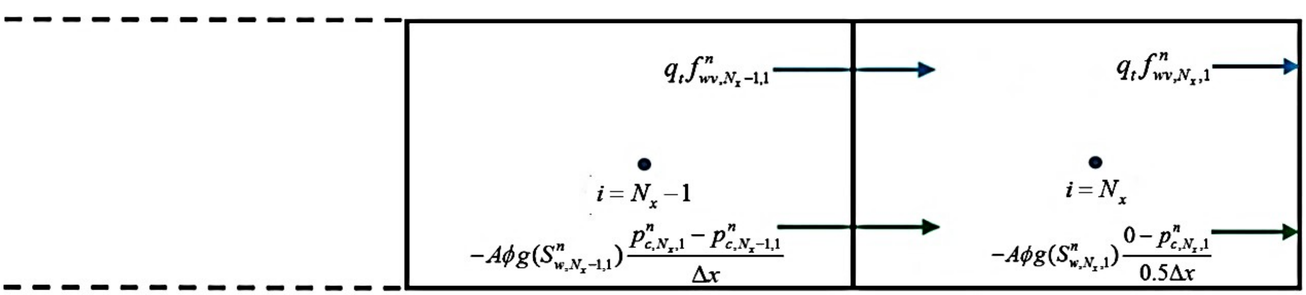

Fig. A3. Water flowrate into the last grid-block due to advection and capillary action.

The important point here is that at the outlet, either no water flows out or water outflow is positive. Negative water outflow should not be allowed, therefore **whenever water outflow from the outlet, Eq. (A20), becomes negative, it is automatically reset to zero**.

$$q_{w,out} = q_t f_{wv,N_x,1} - A\phi g\left(S_w\right)^n_{N_x,1} \frac{0 - p^n_{c,N_x,1}}{0.5\Delta x} \tag{A20}$$

As mentioned before, $g(S_w)$ is always negative, therefore the second term in the water outflow equation is always positive (in water-wet systems) which means capillary action tends to hold water back in the system and not let it flow out. When water reaches the last real grid-block and water starts rising in this grid-block, the term $q_t f_{wv,N_x,1}$ is still very low and the term $-A\phi g\left(S_w\right)^n_{N_x,1}\left(0 - p^n_{c,N_x,1}\right)/(0.5\Delta x)$ is a large negative value and this makes the water outflow negative. It is during this time that water outflow is automatically reset to zero in the code. This accumulates water in the last grid-block in water-wet systems as water is allowed to enter this grid-block but is prevented from flowing out because of capillary action.

In oil-wet systems, the second term in the water outflow equation, Eq. (A20), is always negative which means capillary action favours water flow as soon as it enters the last grid-block, thus a depletion occurs in the water saturation in the last grid-block.

In mixed-wet systems, water accumulates until water saturation reaches a value at which capillary pressure is zero. After that, water depletes in the last grid-block. Note that positive capillary pressure gradient is set by the oil-wet (or mixed-wet) rock but actually generated/provided by the injection pump at the inlet of the system.